Int. J. Multiphase Flow Vol. 6, pp. 51–67
Pergamon/Elsevier, 1980. Printed in Great Britain

SOME CONDENSATION STUDIES PERTINENT TO LWR SAFETY

S. G. BANKOFF

Chemical Engineering Department, Northwestern University Evanston, IL 60201, U.S.A.

Abstract—A number of recent studies involving steam in contact with fairly thick layers of cold water are reviewed. Although most are still largely empirical in nature, some progress has been made in developing liquid-phase turbulence-centered models for condensation in stably-stratified systems. However, instabilities leading to large and rapid variations of heat transfer coefficient are still poorly understood.

1. INTRODUCTION

In the hypothetical LOCA sequence steam comes into contact with cold water in several locations, such as the PWR downcomer, mixing tee and upper plenum, and in the BWR pressure suppression pool. In addition, PWR steam generator waterhammer, due to bubble collapse in the feedring or preheater, represents a potential safety problem. The system behavior in each case is highly dependent upon the local condensation rates. Local condensation rates onto thin liquid films nearly at the saturation temperature in a variety of configurations have been studied extensively, both theoretically and experimentally, and several good reviews are available (Merte 1973; Collier 1972; Butterworth & Hewitt 1977). However, the newer applications mentioned above involve contact of steam with fairly thick layers of cold water. Unsteady behavior, coupled with rapid variation of apparent heat transfer coefficient by several orders of magnitude, is observed under some conditions, and is at present very difficult to predict. On the other hand, steady-state stratified flows may be expected to exhibit similarities to the corresponding flows without condensation (or with small mass transfer, such as absorption of a slightly soluble gas). Even here the analogy is far from exact, since the steam velocity usually decreases rapidly with axial distance, owing to condensation, so that a fully-developed flow is never attained. Attention is first given to steady-state turbulent stratified flows, for which useful information may possibly be extracted from heat and mass transfer studies under similar circumstances, and which can therefore be used as a beginning towards a turbulence-centered model for condensation. Following this development some bubble collapse studies, particularly as applied to reactor safety, are considered. The interesting topics of countercurrent steam–cold water flow and downcomer hydrodynamics are treated elsewhere in this workshop (Block 1979).

2. TURBULENT GAS ABSORPTION MODELS

In developing turbulence-centered models for steam condensation, it is useful to consider first the extensive literature on gas absorption in turbulent liquids. Since the feedback of the mass transfer on the interface motion is not significant in these cases, one can expect that these results will be applicable to one-component condensation primarily for low subcoolings and/or surface shear stresses.

We begin with the two-film model of Lewis (1916) and Whitman (1923), which assumes the existence of laminar films on the gas and liquid sides of the interface, through which mass transport occurs by molecular diffusion. Assuming that the liquid film resistance dominates, the mass transfer coefficient, k_L, is then proportional to the liquid-phase diffusivity, D_L. Higbie

(1935) proposed a penetration theory, in which packets of fresh liquid arrive at the interface, receive added mass by molecular diffusion, and then are returned to the bulk liquid after an exposure time, t_e. This leads to a mass transfer coefficient proportional to $D_L^{1/2}$. Subsequent refinements by Danckwerts (1951) (distribution function for exposure times); Dobbins (1956) (finite thickness of renewal element); Kishinevskii (1949) (turbulent diffusivity added to the molecular diffusivity); and King (1966) (turbulent diffusivity varying as a power-law of distance from the interface) led to successively more complex parametric models.

Fortescue & Pearson (1967) suggested that the liquid is brought to the surface in the form of large eddies. The convective transport equation is then

$$u_1 \frac{\partial C}{\partial x} + v_1 \frac{\partial C}{\partial y} = D_L\left(\frac{\partial^2 C}{\partial x^2} + \frac{\partial^2 C}{\partial y^2}\right), \qquad [1]$$

where a periodic, square, two-dimensional eddy structure is assumed at the surface, leading to

$$u_1 = U \sin\frac{\pi x}{L}\cos\frac{\pi y}{L}, \qquad [2]$$

$$v_1 = U \cos\frac{\pi x}{L}\sin\frac{\pi y}{L}. \qquad [3]$$

Here U is the maximum velocity in the eddy, x and y are the coordinates parallel and normal to the interface, respectively, and L is the eddy size, taken to be the integral scale of turbulence, λ_t. It is also assumed that U is proportional to the turbulent intensity, u_t. Solution of the transport equation with periodic boundary conditions in the x-direction leads to

$$k_L = 1.46\left(\frac{D_L u_t}{\lambda_t}\right)^{1/2}. \qquad [4]$$

Banerjee *et al.* (1968) and Lamont & Scott (1970), on the other hand, considered that small eddies may dominate the transport process. The velocity amplitude then becomes dependent on the wave number, n:

$$U \sim (nE(n))^{1/2}, \qquad [5]$$

where $E(n)$ is the energy spectrum for fully-developed turbulence, approximated by a formula due to Kovasznay (1967). Upon integrating with respect to wave number the result was

$$k_L \sim \left(\frac{D_L^2 \varepsilon}{\nu_L}\right)^{1/4}, \qquad [6]$$

where ε is the dissipation rate per unit mass.

Levich (1962) took into account the variation in surface elevation due to arrival of an eddy at the interface, balancing the capillary pressure against the turbulent pressure intensity due to the large eddies. The resulting expression was

$$k_L = \left(\frac{D_L \kappa}{\sigma}\rho_L u_t^3\right)^{1/2}, \qquad [7]$$

where σ is the surface tension and κ is the von Karman constant (0.4).

Brumfield *et al.* (1975, 1976) examined several sets of mass transfer data, and presented a

synthesis of the large-eddy (inertial range) and small-eddy (dissipative range) models:

$$k_L = 0.25\sqrt{D_L}\left(\frac{u_t^3}{\nu\lambda_t}\right)^{1/4} \qquad \mathrm{Re}_t > 500, \tag{8}$$

$$k_L = 0.7\,F(\tau_e)\left(\frac{D_L u_t}{\lambda_t}\right)^{1/2} \qquad \mathrm{Re}_t < 500, \tag{9}$$

where $\tau_e = t_e u_t/\lambda_t$, dimensionless exposure time for a single eddy and $F(\tau_e)$ = weakly varying function, given by figure 1 (Brumfield *et al.* 1975) such that $F(\tau_e) = 1 + 0.44/\tau_e$ for $\tau_e > 0.85$ and $\mathrm{Re}_t = \lambda_t u_t/\nu$, turbulent Reynolds number.

It is readily found that the analogous dimensionless heat transfer equations are (Bankoff 1978; Thomas 1979)

$$\mathrm{Nu}_t = 0.25\,\mathrm{Re}_t^{3/4}\,\mathrm{Pr}^{1/2} \qquad \mathrm{Re}_t > 500, \tag{10}$$

$$= 0.7\,F(\tau_e)\,\mathrm{Re}_t^{1/2}\,\mathrm{Pr}^{1/2} \qquad \mathrm{Re}_t < 500, \tag{11}$$

where the turbulent Nusselt number is given by $\mathrm{Nu}_t = h_L\lambda_t/k_l$. Here h_L is the interfacial heat transfer coefficient in the absence of condensation, and must be corrected for condensation, as discussed later. The small-eddy equation [10] may involve some error for heat transfer, because $\mathrm{Pr} \ll \mathrm{Sc}$ for liquids (Theofanous 1979; Banerjee 1979).

Thomas (1979) has extended these results in a two-layer model. Immediately adjacent to the free surface it is assumed that there is a viscous layer, of thickness δ_s, whose thermal resistance is expressed by a heat transfer coefficient, h_s. Beneath the viscous layer the eddy heat transfer coefficient is of the form $\gamma_1 c_L \rho_L u_t y/\lambda_t$, where y is the distance from the free surface and γ_1 is a constant of order unity. The overall coefficient is then given by

$$\frac{1}{h_L} = \frac{1}{h_s} + \frac{1}{\gamma_1 c_L \rho_L u_t}\ln\left(\frac{\gamma_2\lambda_t}{\delta_s}\right), \tag{12}$$

where it has been assumed that the bulk temperature is attained at a distance $\gamma_2\lambda_t$ from the free surface. Using a formula due to Longuet-Higgins (1960) for oscillatory free-surface boundary layers:

$$\delta_s \sim \gamma_3\left(\frac{\nu\lambda_t}{u_t}\right)^{1/2}, \tag{13}$$

where γ_3 is another constant of order unity. Thus

$$\frac{1}{h_L} = \frac{1}{h_s} + \frac{1}{\gamma_1 c_p \rho_l u_t}(B + \ln \mathrm{Re}_t^{1/2}), \tag{14}$$

where $B = \ln(\gamma_2/\gamma_3)$. To estimate h_s, [10] is used, with no correction for mass transfer effects. This point will be discussed later.

Tsacoyannis (1976) and Masbernat (1977) have studied the effect of surface waves in the absorption of O_2 and CO_2 in a horizontal stratified concurrent flow. Following the small-eddy model, and taking $\varepsilon = u_t^3/\lambda_t$, the Lamont-Scott formula is employed in dimensionless form:

$$\frac{k_L}{u_{sf}} = \gamma_4\,\mathrm{Sc}^{-1/2}\,\mathrm{Re}_L^{-1/4}, \tag{15}$$

where u_{sf} is the friction velocity on the liquid side of the gas–liquid interface; Sc is the Schmidt number; and the local Reynolds number is evaluated by two different formulas, depending on the surface wave height:

(1) For relatively small waves, identified by $a/d < 0.2$, where d is the liquid depth and a is the effective surface roughness height, it is assumed that $u_t \sim u_L$, and $\eta/\lambda_t \sim a/d$, where η is the Kolmogoroff microscale, given by

$$\eta = \lambda_t \, \mathrm{Re}_t^{-3/4}.$$

Thus, for $a/d < 0.2$ or $u_L a/\nu_L < 100$,

$$\mathrm{Re}_L = \gamma_5 (a/d)^{-4/3}. \qquad [16a]$$

(2) If $a/d > 0.25$ or $u_L \, a/\nu_L > 100$,

$$\mathrm{Re}_L = u_L \, a/\nu_L \qquad [16b]$$

which corresponds to the hypothesis that $\lambda_t \sim a$.

The experimental data were fitted over a liquid Reynolds number range $\mathrm{Re}_L = 70$–7000 by this composite model, using $\gamma_5 = 13$; $\gamma_4 = 0.55$ (figure 1).

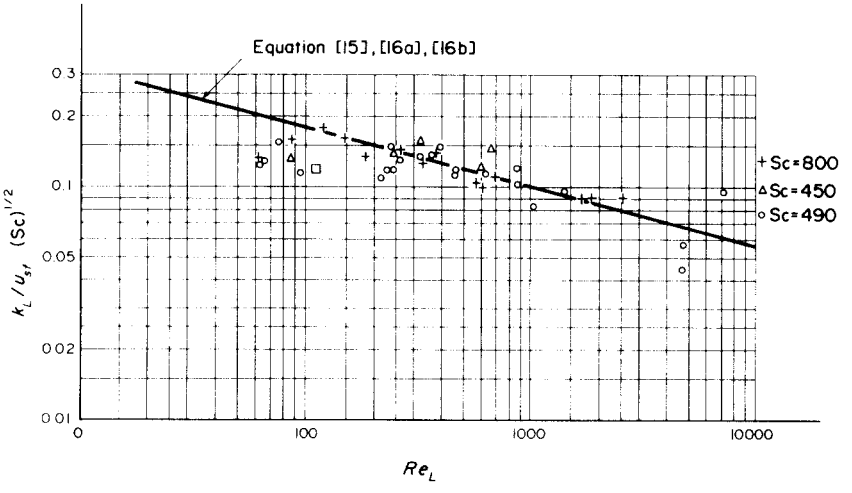

Figure 1. Comparison of experimental results of Tsacoyannis (1976) and Masbernat (1977) with [15] and [16].

3. CORRECTIONS FOR CONDENSING MASS TRANSFER

Except under highly transient or intense surface shear conditions, the principal resistance to condensation heat transfer, in the absence of air, is on the liquid side. However, it is necessary to correct the formulas obtained in gas absorption or non-condensing heat transfer for the effect of the normal surface velocity induced by condensation. In the absence of heat transfer data the Colburn analogy (1933) can be used as a rough guide to estimate heat transfer rates from pressure drop or mass transfer data. The Silver–Wallis correction factor (1965–66) was used, for example, by Linehan *et al.* (1969) who measured the local surface temperature and the temporal mean film thickness in cocurrent stratified flow of saturated steam over a thin (~0.1 cm) subcooled water film:

$$\frac{f_i^*}{f_i} = \varphi + \mathrm{e}^{-\varphi/2}, \qquad [17]$$

where f_i^* and f_i are the interfacial friction factors with and without condensation, and

$$\varphi = \frac{2m}{\rho_g u_{gr} f_i} = \frac{m u_{gr}}{\tau_i}, \qquad [18]$$

is the ratio of the Reynolds momentum flux, mu_{gr}, and the interfacial shear stress in the absence of condensation, τ_i. Here m is the condensing mass flux and $u_{gr} = u_g - u_i$ is the velocity of the gas stream relative to the interface velocity. Alternatively, Mickley *et al.* (1954) used the Whitman film theory to obtain

$$\frac{f_i^*}{f_i} = \frac{\varphi}{1 - e^{-\varphi}}, \qquad [19]$$

which is identical to [17] for $\varphi \gg 1$ and $\varphi \ll 1$. Spalding (1963) arrives at an equation similar to [19] by a somewhat different method. Mickley also obtains

$$\frac{h_L^*}{h_L} = \frac{\varphi_H}{1 - e^{-\varphi_H}} \cong 1 - \varphi_H; \; \varphi_H = \frac{mc_p}{h} = \frac{c_p \Delta T_{sub}}{h_{fg}}, \qquad [20]$$

where h_L^* is the heat transfer coefficient in the presence of condensation. The positive sign of the correction term should be noted. In the usual case of heat transfer from a porous hot wall, heat transfer is reduced by blowing and enhanced by suction. Here the principal heat transfer resistance is on the liquid side, and condensation induces a blowing effect on the liquid. However, the liquid is colder than the interface, so that the blowing enhances the heat transfer. At the present time this approach has not been verified for steam–water condensation, since no data exist for identical flow conditions with and without condensation.

4. STRATIFIED HORIZONTAL CONDENSING FLOWS

Bankoff *et al.* (1978) and Lee *et al.* (1979) measured local steam condensation rates in a cocurrent horizontal stratified flow of steam and subcooled water in a 305 mm × 64 mm rectangular channel 1.56 m long (figure 2). Electrically-heated pitot tubes were used to measure steam mass flow rates at four locations along the centerline. Two dimensional effects were

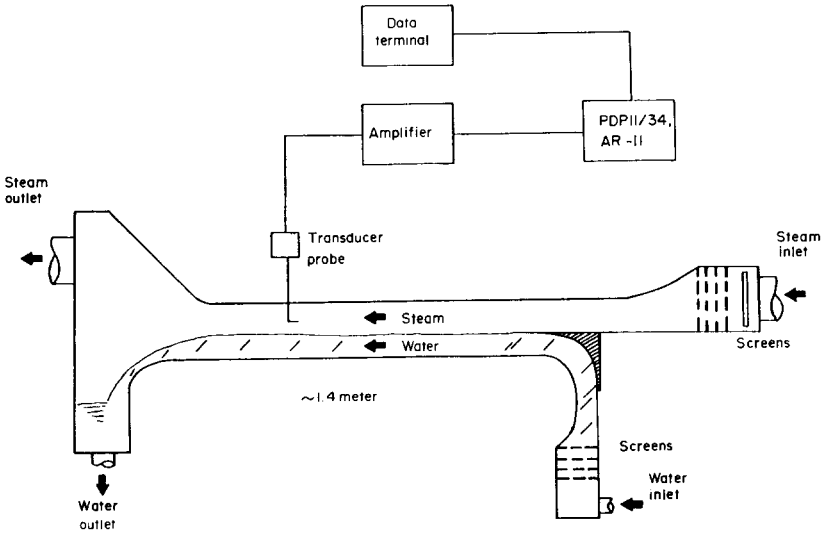

Figure 2. Schematic of horizontal channel for cocurrent steam–water stratified flow (Bankoff *et al.* 1978; Lee *et al.* 1979).

taken into account by calibrating each pitot tube against the venturi measurement under conditions of negligible condensation. The correction ranged from +14 to −6 per cent, depending on the location and the mass flow rate. The measured air content of the steam was about 4 ppm. In addition to the axial steam flow profile, the inlet water and steam flow rates, the inlet and outlet water temperatures, and the depth of the water layer along the channel were also measured.

Typical steam mass flow rates as a function of axial position are shown in figures 3–5. The experimental data indicate that the local condensation rate increases with increasing steam flow rate, water flow rate and the degree of subcooling.

The average heat transfer coefficients of the data shown in figure 3 are shown in figure 6. For each run, $\bar{h}_x$ is fairly constant, despite the nearly five-fold decrease in steam velocity over the channel length.

The experimental data can be correlated by defining the Stanton number, $\overline{\mathrm{St}}_L$ as a function of liquid Reynolds number ($\overline{\mathrm{Re}}_L$) and vapor Reynolds number ($\overline{\mathrm{Re}}_G$)

$$\overline{\mathrm{St}}_L = \frac{\bar{h}_x}{c_L G_L},$$

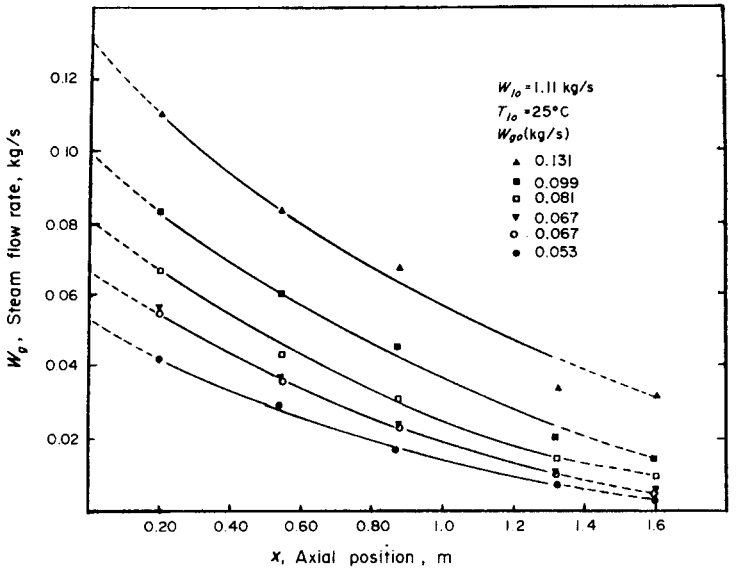

Figure 3. Axial steam flow rates as function of inlet steam flow rate in horizontal channel.

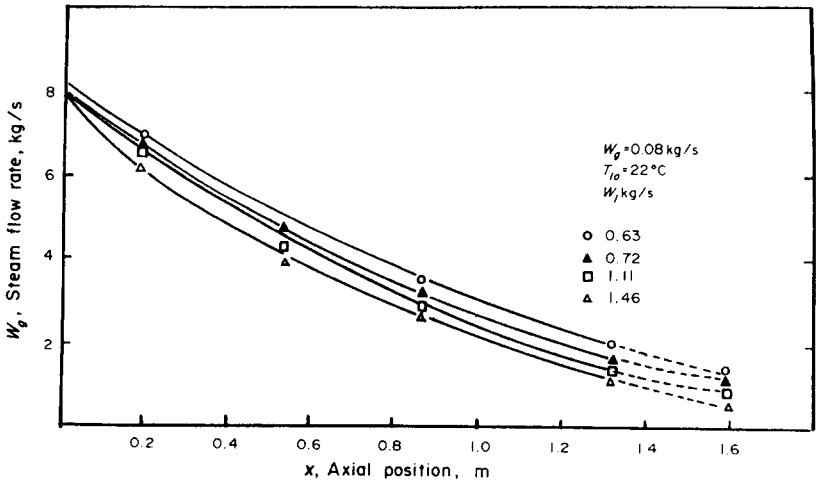

Figure 4. Axial steam flow rates as function of inlet water flow rate in horizontal channel.

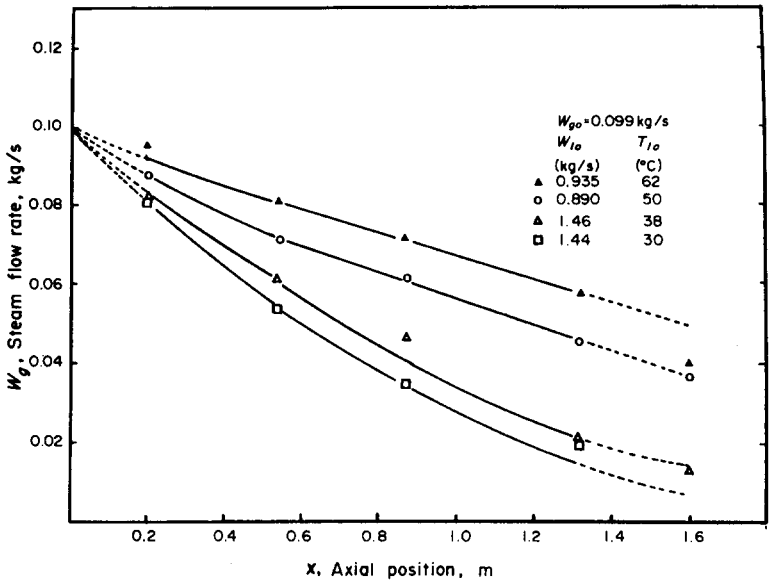

Figure 5. Axial steam flow rates as function of inlet water temperature in horizontal channel.

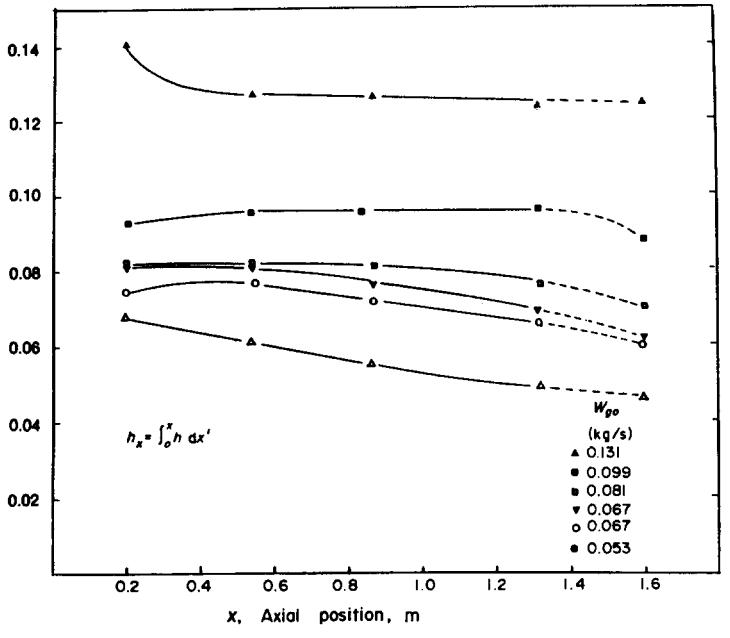

Figure 6. Axial average heat transfer coefficient as function of steam flow rate in horizontal channel.

and

$$\overline{\mathrm{Re}}_L = \frac{\bar{G}_L x}{\mu_L},$$

$$\overline{\mathrm{Re}}_G = \frac{\bar{G}_L x}{\mu_G},$$

where $\bar{G}$ is the average of the inlet and local mass velocities at the distance x from the entrance, and $\bar{h}_x$ is a local heat transfer coefficient, averaged from the entrance.

As shown in figure 7, the correlation can be expressed as

$$\overline{\mathrm{St}}_L = 0.0045\,\overline{\mathrm{Re}}_G^{1/3}\,\overline{\mathrm{Re}}_L^{-0.29}. \qquad [21]$$

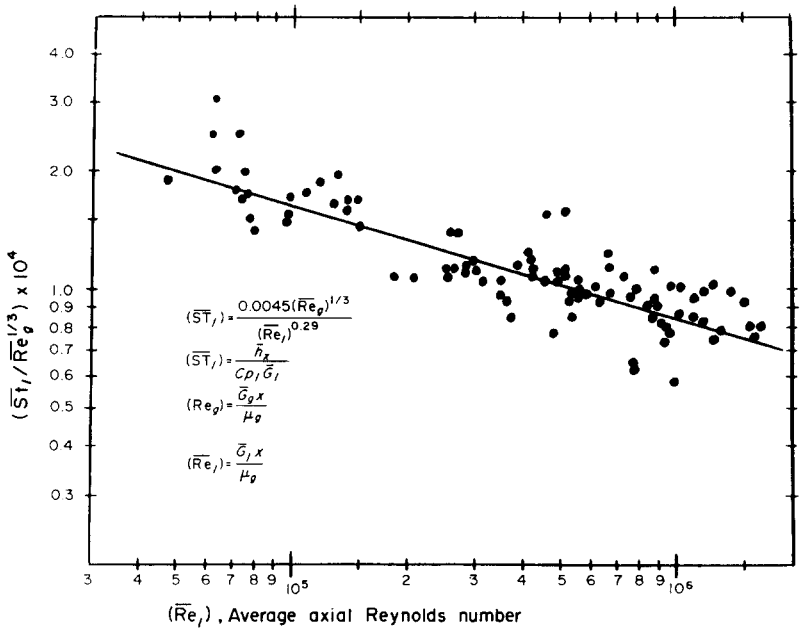

Figure 7. Correlation of Stanton Number as function of water and steam Reynolds Numbers in horizontal channel.

It is interesting that the dependence upon x does not appear explicitly, since this can be written in the form

$$\overline{St}_L \cong 0.0045 \left(\frac{\bar{G}_G \mu_L}{\bar{G}_L \mu_G}\right)^{1/3}. \qquad [22]$$

In fact, both $\bar{G}_G$ and $\bar{G}_L$ are functions of x, due to condensation, on the one hand, and to variations in surface shear and hydrostatic head on the other. Decreases in G_G by a factor of five or more imply that the local acceleration pressure gradient is significant, which makes the evaluation of the interfacial friction velocity difficult, and also implies that the flow is never fully developed.

Thomas (1979) examined a variety of flow configurations, including a vertical water jet impinging on the free surface from below, grid turbulence decaying in an open channel, and recirculating flows generated by submerged horizontal jets. The grid channel data were obtained in a horizontal channel, 100 mm × 100 mm in cross-section and 1.09 m long, fitted with a turbulence-promoting square grid at the liquid entrance. In contrast to the channel condensation experiments of Bankoff *et al.* (1978), the steam velocity was everywhere nearly zero, since steam was supplied at both ends at a rate sufficient to maintain a constant pressure (0.43–0.95 bar). It was shown that flow patterns in the steam space had no effect on the condensation rate. Based on hot-film anemometer measurements and surface flow visualizations, it was suggested that the appropriate velocity and length scales of the turbulence were:

	u_L	λ_t
$0 < x/L < 0.15$	$0.40\, u_t$	m,
$0.15 < x/L < 1$	$0.15\, u_t$	d,

where u_L is the mean liquid velocity; m is the grid mesh (12.7 mm); and L is the channel length. For the data in this geometry $(\rho_L c_L u_t) \sim 52$, while the measured value of $\bar{h}_L \sim 0.66$ kW/m² K. Therefore, $\bar{h}_L \sim h_i$ the viscous sublayer (small eddy) heat transfer coefficient calculated from [10], which was 1.56 kW/m² K. Hence the predicted value was high by a factor of 2.4. On the

other hand, the predicted and measured heat transfer coefficients were in agreement within a factor of less than two in experiments with the horizontal channel containing submerged water jets which agitated the surface layers. In this channel the water entrance and drawoff were both submerged in the lower half of the water layer, and the surface shear stress was negligible, so that the above estimates of the turbulent intensity near the surface may have been high by a factor of two or three. In the experiment of Bankoff *et al.* (1978), the steam velocity was always large compared to the liquid even after 80% condensation (~30 m/s vs ~ 1 m/s for steam vs water entrance velocities). Furthermore, the water discharge into the exit plenum was governed by critical open-channel flow. In this case, choosing $u_t = 0.3\ u_L$, $\lambda_t = d$ results in a reasonable fit of the measured $\bar{h}_L$ and the value predicted by [10], as shown in figure 8. The use of turbulence-centered models thus appears to be promising, although much additional work is needed.

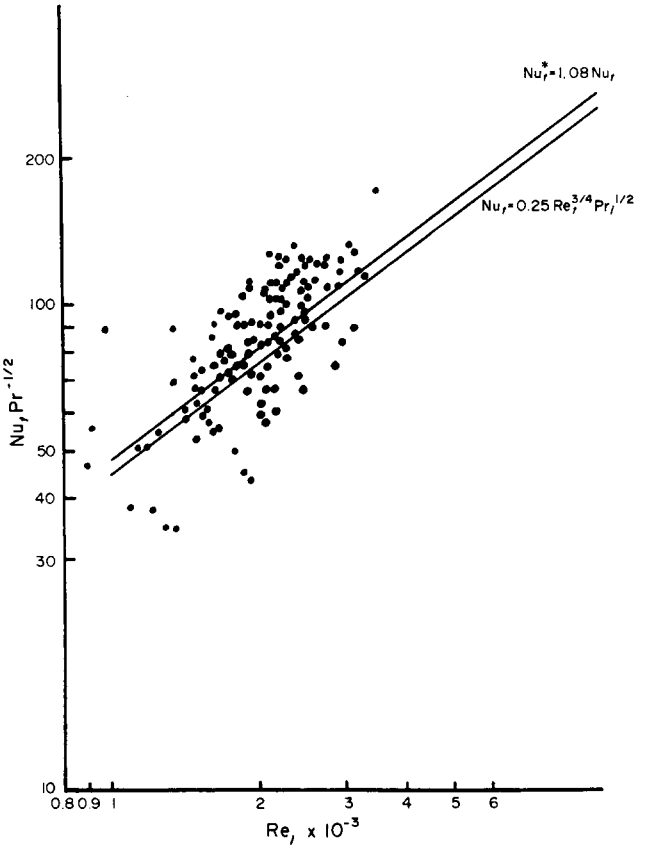

Figure 8. Comparison of [10] with and without correction for mass transfer using [20] with data in horizontal channel.

5. STEAM BUBBLE COLLAPSE

Steam bubble collapse leads to waterhammer effects, which represent potential problems for PWR steam generators and for BWR pressure suppression pools. Collapse of small entrained steam bubbles may also be a fundamental process in the rapid mixing of steam and cold water during the ECCS sequence. The collapse of small isolated steam bubbles is almost always governed by the thermal and internal resistance of the surrounding liquid, although in cases where intense shear is encountered, the steam-side non-equilibrium thermal resistance can become significant. Small amounts of air in the steam can also cause the steam-side thermal resistance to dominate.

The well-known Rayleigh solution is a useful approximation for the collapse of a spherical bubble in highly subcooled water. In this case, particularly at low pressures, the condensation

rate is so large during the initial stage of collapse that the bubble can be considered to be virtually empty, so that collapse proceeds under constant pressure difference. At low subcoolings and/or high pressures, together with laminar flow, however, the thermal resistance of the liquid boundary layer at the bubble surface cannot be ignored. The integral boundary layer method, in which a quadratic temperature profile is assumed in the thin thermal boundary layer, has been used by Theofanous *et al.* (1969) to calculate bubble growth and collapse in the combined inertial-thermal regime. While this method gives generally good results, it must be remembered that in the collapse phase the volume of the liquid thermal boudnary layer increases with time, while the bubble volume decreases. One can expect therefore that the thin thermal boundary layer assumption will fail when the two volumes become approximately equal.

The effects of bubble translation on bubble collapse were studied by Wittke & Chao (1967), at various values of reduced gravity, for small subcoolings ($\leq 10°C$). The measured radius-time were in satisfactory agreement with their numerical solution of the conservation equations.

Moalem & Sideman (1973) treated the collapse of a single bubble containing either pure steam or a steam–air mixture, translating through subcooled liquid. For pure steam the volume vs time relationship could be written in the form:

$$\left(\frac{V}{V_{\max}}\right)^{1/2} = C_1 + C_2\,\mathrm{Fo}_m, \qquad [22]$$

where $V_{\max}$ is the maximum bubble volume; $\mathrm{Fo} = \alpha_f t/R_m^2$; R_m is the maximum bubble radius; and C_1 and C_2 are functions of the system parameters. The work was extended by Moalem *et al.* (1973) to include condensation of a bubble train, again by potential flow methods. Brucker & Sparrow (1977) measured the collapse of small (~3 mm) single bubbles rising in a quiescent subcooled pool of water at pressures of 10–62 bars and subcoolings of 15–100 K. A constant rise velocity was observed, in agreement with earlier observations (Moalem & Sideman 1973), and the dimensionless time to collapse (Fourier number) was correlated by the Jakob and Rayleigh numbers:

$$\mathrm{Fo} = 55.5\quad \mathrm{Ja}^{-3/4}\quad \mathrm{Ra}^{-1/2}, \qquad [23]$$

where $\mathrm{Fo} = \alpha_L t_c/R_0^2$; $\mathrm{Ja} = \rho_L c_L \Delta T_{\mathrm{sub}}/\rho_G h_{fg}$; and $\mathrm{Ra} = [g(\rho_L - \rho_G)\ D_0^3/\rho_0^3/\rho_L \nu_L^2]\,\mathrm{Pr}_L$. Here t_c is the time to collapse; R_0 and D_0 are the initial bubble radius and diameter, respectively; and liquid properties were evaluated at $T_L = \frac{1}{2}(T_{\mathrm{sat}} + T_\infty)$. Average heat transfer coefficients over this broad range of operating conditions were 10 kW/m^{2}K within ± 50 per cent, which is a notable result.

On the other hand, under highly turbulent conditions remarkably high transfer coefficients may exist. Bankoff & Mason (1962) injected steam through a small hole (0.5–1.75 mm exit diameter) into a cold water jet impinging on a flat plate, and photographed the oscillating steam bubble with a Fastax camera in order to determine the time-mean interfacial area. Bubble frequencies ranged from $2 \times 10^2 - 2 \times 10^3\ \mathrm{sec}^{-1}$, and the heat transfer coefficients from 7 to 1800 kW/m^{2}K, depending on the water temperature and jet velocity, and steam flow rate. The higher values indicate the virtual absence of a laminar sublayer at the steam–water interface. Similar values were obtained in fitting experimental pressure distribution in the mixing chamber of jet injectors to analytical models by several investigators (Rose 1960; Linehan & Grolmes 1970; Levy & Brown 1967). Under these conditions the approach velocity of the condensing steam $\sim 10^{-2}$ m/s (Mach number ~0.3), so that the interphase mass transfer resistance is very significant, and a kinetic theory approach for limiting condensation rates, such as that of Marble & Shankar (1971), is necessary.

A linearized analysis due to Schrage results in the following expression relating the

condensing mass flux to the non-equilibrium temperature and pressure driving forces:

$$m = \left(\frac{1}{2\pi R_\gamma T_i}\right)^{1/2} \left(\frac{2\sigma}{2-\sigma}\right) P_i \left(\frac{P_{sat} - P_i}{P_i} - \frac{T_{sat} - T_i}{2T_i}\right), \quad [24]$$

where σ = accommodation coefficient, ranging from 0.01 to 1 in reported values for water; R_γ = gas constant, mass units; T_i = temperature of liquid–vapor interface; T_{sat} = saturated vapor temperature; P_i = vapor pressure at liquid–vapor interface temperature; and P_{sat} = bulk vapor pressure.

A simplified form which has been used for rapid condensation (Kowalchuk & Sonin 1978) is:

$$m = \sigma \rho_{sat} \left(\frac{R_\gamma T_{sat}}{2\pi}\right)^{1/2}, \quad [25]$$

which states that the mass flux is a fraction of the mean mass flux due to thermal motions of the gas molecules, and σ is said to be the fraction of the vapor molecules hitting the liquid surface which stick. In fact, as used by these authors, σ is an empirical correction factor, taken arbitrarily to be ~0.8.

The reported values of the accommodation coefficient, σ, range from 0.04 to 1 for water. Wilcox & Rohsenow (1970) have examined the available data, and conclude that $\sigma \sim 1$, with the lower reported values due to the difficulty in making accurate surface temperature measurements and excluding all traces of non-condensable gases.

It is interesting to compare the very high heat transfer coefficients found by Bankoff & Mason (1962) with [10]. An appropriate turbulent Reynolds number takes $\lambda_t = d_0$, the injection hole diameter and $u_t = 2d_0/\omega_b$, where ω_b is the bubble frequency. Taking $d_0 = 1.75$ mm and $\omega_b = 2 \cdot 10^3\ s^{-1}$, one obtains $h = 1050\ \mathrm{kW/m^2K}$, which is in the right range with the reported average heat transfer coefficient. Greef (1975) and Cumo *et al.* (1978) have also measured large heat transfer coefficients ($\sim 10^3\ \mathrm{kW/m^2K}$) in steam injection into cold water. Sursock & Duffey (1978) have used the Greef data to construct a dynamic model for the "chugging" of a BWR pressure suppression pool, which agrees with collapse time data taken in small-scale and full-scale facilities. There seems to be no doubt, therefore, that $\bar{h}$ can exhibit variations of two orders of magnitude when steam and cold water are brought into contact. Further, these transitions can occur quite rapidly, leading to water hammer and/or surface instabilities.

The purpose of the Bankoff & Mason study (1962) was a simulation of bubble dynamics in subcooled nucleate boiling. The conclusion was drawn that latent heat transport within the bubble accounts for most of the heat transfer from the wall in subcooled nucleate boiling, based on comparisons with bubbles observed by Gunther & Kreith (1950). Recently Plesset & Prosperetti (1978) have employed a highly simplified model of the microlayer beneath the bubble to conclude that latent heat transport accounts for a small share of the total heat transfer, but their physical assumptions are questionable. A simple calculation, using these enormous heat transfer coefficients on the upper bubble surface, leads quickly to the conclusion that the bubbles in high-shear highly-subcooled nucleate boiling act as heat pipes with very low internal transfer resistance. Greef (1975) similarly calculated that only 2–3 per cent of the total steam flow rate in his pool injection experiment appears as visible bubbles.

6. PRESSURE SUPPRESSION POOL STUDIES

Injection of steam into a cold-water pool through a vertical downcomer, which occurs in the BWR pressure suppression pool, can result in "chugging", due to bubble growth and collapse. The resulting tank wall stresses can be significant.

6.1 *KONDAS model (Class 1977)*

Class notes that turbulence can be generated in the vicinity of the bubble simply by the oscillating movements of the water level, without a pronounced net flow, which in turn affects the mass transfer, and results in a feedback loop. In the KONDAS computer program developed at Karlsruhe a first model was based on surface renewal at a frequency ω, analogous to the large eddy model of Fortescue and Pearson, giving in the simplest form:

$$h_L = 2\left(\frac{k_L \rho_L c_L \omega}{\pi}\right)^{1/2}. \qquad [26]$$

However, values about two orders of magnitude for ω higher than the large-eddy concept (~100 Hz) would imply had to be introduced in order to fit experimental data. Further, experiments on large vapor bubbles indicate that the simple equation is inadequate, since the condensation rate may suddenly rise during the bubble collapse, indicating that cold water is reaching the surface of the bubble. This is due to the tangential flow induced during bubble formation and collapse. The KONDAS program therefore uses a feedback model in which the turbulence is excited by the flow conditions at the interface. This feedback is said to give satisfying results within the range of expected frequency of about 100 Hz.

In addition, the surface area is calculated by a statistically-treated roughening multiplier, reflecting the irregular condition of the bubble surface. Further, it seems possible that the eddy diffusivity normal to the surface will be affected by rapid bubble collapse.

6.2 *Kowalchuk & Sonin model*

Kowalchuk & Sonin (1978) take a simplified form for the eddy diffusivity for heat:

$$\alpha_T = \beta \bar{u}_b D, \qquad [27]$$

where β is an empirical coefficient, expected to be of order 10^{-2}, $\bar{u}_b$ is the time-averaged mean flow speed in one oscillation cycle, and D is the pipe diameter. On this basis, using a simple transient conduction solution, the heat flux into the water for the period when the interface is inside the pipe is given by

$$q = \rho_L c_L \sqrt{\frac{\beta \bar{u}_b D}{t_0 + t}} (T_{\text{sat}} - T_L), \qquad [28]$$

where the time t is measured from the instant of entry into the pipe, and t_0 is an artificial delay time, given by

$$t_0 = \alpha_T \left(\frac{\rho_L c_L (T_{\text{sat}} - T_L)}{q_0}\right)^2, \qquad [29]$$

where q_0 is the heat flux just before the interface enters the pipe. When the interface is pushed outside the pipe, cold water is entrained from the pool, and the heat flux density jumps to a higher value. Assuming that the thermal boundary layer scales as the pipe diameter, one can derive

$$q = \text{St}_c \rho_L c_L \bar{u}_b (T_{\text{sat}} - T_L), \qquad [30]$$

where St_c is an empirical constant, which can be identified as a "condensation Stanton

number", suggested to be of order 10^{-1}. Combining these equations they obtain

$$q = \frac{\mathrm{St}_c \rho_L c_L \bar{u}_b (T_{\mathrm{sat}} - T_L)}{\left(1 + \dfrac{\delta\pi\ \mathrm{St}_c^{\,2}}{\beta} \cdot \dfrac{\bar{v}t}{D}\right)^2}, \qquad [31]$$

where $\delta = 0$ for interface outside pipe and $\delta = 1$ for interface inside pipe.

6.3 *Sursock & Duffey model* (1978)

This model derives a third-order equation for the interface position, where it is assumed that inside the downcomer, the interface is quiescent and condensation ceases, so that the manometer equation applies. When the interface protrudes below the tube end, the heat transfer coefficient is assumed to be proportional to the liquid subcooling, and rapid condensation occurs. This model is interesting in that the rapid condensation rate is not chosen arbitrarily to fit the data, but instead is developed on the basis of a turbulent transport model and Greef's data. Following Motte & Bromley (1957), the Reynolds flux velocity in turbulent transport near the interface is proportional to $(\alpha_t/t_c)^{1/2}$, where α_t is the turbulent diffusivity and t_c is a characteristic time for eddy transport in the liquid. For bubble collapse, an energy balance at the interface requires that at every instant

$$q = R\rho_G h_{fg} = \frac{\alpha_t \rho_L c_L \Delta T_{\mathrm{sub}}}{(\alpha_t t_c)^{1/2}}. \qquad [32]$$

Integrating from $t = 0$ to $t = t_c$ to obtain an average heat transfer coefficient:

$$\Delta R \rho_G h_{fg} = \rho_L c_L \Delta T_{\mathrm{sub}} (\alpha_t t_c)^{1/2}, \qquad [33]$$

where $\Delta R = R(t_c) - R(0)$. If now ΔR is taken to be a constant for a given system and subcooling, it follows that $h_L \propto \Delta T_{\mathrm{sub}}$. The proportionality constant in the model is determined by reference to the Greef data with a 1.2 mm orifice for bubble frequency vs ΔT_{sub}, taking $h_L \Delta T_{\mathrm{sub}} = 10^5\ \mathrm{kW/m^2}$. There is, of course, a considerable statistical scatter in the time interval between successive "chugs" in any experimental run. Allowing for this scatter, the predicted and experimental chug frequencies are in satisfactory agreement with downcomer diameters varying from 0.12 to 5.1 to 61.0 cm.

7. CONCLUDING REMARKS

This brief review has concentrated on condensation of steam in contact with a fairly thick body of cold water. The essential features which have been discussed are the following:

(1) A beginning has been made in the application of turbulent transport theory to the prediction of condensation heat transfer coefficients. In particular, the heat transfer analog of the Brumfield *et al.* mass transport equation (1976), based on free-surface gas absorption data, is reasonably successful in predicting average condensation coefficients for several sets of horizontal open-channel flow (Bankoff *et al.* 1978; Thomas 1979), as well as turbulent free jets and submerged jets Thomas 1979); and by proper choice of the characteristic time and velocity scales, the extremely high heat transfer coefficients (approximately two orders of matnitude greater) observed with a small steam jet issuing into a high-shear subcooled liquid region (Bankoff & Mason 1962). Further, by rational choice of scales, direct evaluations of the turbulent heat flux have led to reasonable agreement with chugging frequency data over a wide range of characteristic dimensions (Surcock & Duffey 1978).

(2) The very large condensation coefficients are not as well understood at this time, but may

be associated with surface instabilities, as well as rapid eddy transport directly to the interface. In this connection one can note the observation of Gardner & Crow (1973) of a critical Kutateladze number for steam bubble entrainment, and of Reynolds & Berthoud (1978) of the necessity for a turbulent two-phase mixing layer in order to model correctly the collapse rates of large bubbles, produced by breaking a glass sphere containing superheated water, immersed in a tank of cold water.

NOMENCLATURE

- a effective wave roughness height
- c_L specific heat of liquid
- C concentration
- $C_{1,2}$ constants
- d water layer depth; hole diameter
- D molecular diffusivity; pipe diameter
- f_i interfacial friction factor
- Fo Fourier number, [23]
- $\bar{G}$ mass velocity
- h interfacial heat transfer coefficient
- h_{fg} latent heat of evaporation
- h_s heat transfer conductance of surface viscous layer
- Ja Jakob number, [23]
- k_L mass transfer coefficient; thermal conductivity
- L characteristic length, [2] and [3]; length of horizontal channel
- m condensation mass flux
- Nu Nusselt number
- P pressure
- Pr Prandtl number
- q heat flux
- R bubble radius; gas content
- Ra Rayleigh number, [23]
- Re Reynolds number
- Sc Schmidt number
- T temperature
- t time
- u velocity parallel to surface
- u_{sf} friction velocity
- u_t turbulent intensity
- U velocity amplitude
- V volume
- x coordinate parallel to flow
- y coordinate normal to flow
- α_L molecular thermal diffusivity
- α_t turbulent diffusivity
- β empirical coefficient, [27]
- $\gamma_{1,2,3,4,5}$ constants, [12]–[16]
- δ boundary layer thickness
- ε dissipation rate per unit mass
- λ_t integral scale of turbulence
- φ defined by [18]
- κ Von Karman universal constant

η Kolmogoroff length scale
μ viscosity
ν kinematic viscosity
ρ density
σ accommodation coefficient; surface tension
τ shear stress
ω frequency

Subscripts

b bubble
c collapse
e exposure
gr grid
G gas
H heat
i interface
L liquid
m maximum
o initial
r relative
v vapor
sat saturation
sub subcooling
t turbulent
x local value
∞ infinity

Superscripts

— average
* corrected for mass transfer effect

REFERENCES

BANERJEE, S., SCOTT, D. S. & RHODES, E. 1968 Mass transfer to falling wavy liquid films in turbulent flow. *Indust. Engng Chem. Fund.* **7**, 22–26.

BANKOFF, S. G. 1978 Brief literature review pertinent to steam generator water hammer. PWR Steam Generator Water Hammer Workshop, EPRI, Palo Alto, CA.

BANKOFF, S. G. & MASON, J. P. 1962 Heat transfer from the surface of a steam bubble in turbulent subcooled liquid stream. *AIChE J.* **8**, 30–33.

BANKOFF, S. G. TANKIN, R. S & YUEN, M. C. 1978 Steam–water mixing studies. 6th *Int. Light-Water Reactor Safety Information Meeting*, Nuclear Reg. Comm., Gaithersburg, MD.

BANKOFF, S. G. TANKIN, R. S & YUEN, M. C. 1979 Condensation rates in steam–water mixing. Annual Progress Report, NRC.

BLOCK, J. A., 1979 Condensation-driven fluid motions. EPRI Workshop on Two-Phase Flow Modeling in Reactor Safety and Performance, Tampa, FL.

BRUCKER, G. G. & SPARROW, E. M. 1977 Direct contact condensation of steam bubbles in water at high pressure. *Int. J. Heat Mass Transfer* **20**, 371–381.

BRUMFIELD, L. K., HOUZE, R. N. & THEOFANOUS, T. G. 1975 Turbulent mass transfer at free, gas-liquid interfaces, with applications to film flows. *Int. J. Heat Mass Transfer* **18**,

1077–1081; *ibid* 1976 Turbulent mass transfer at free, gas-liquid interfaces, with applications to open-channel, bubble, and jet flows. *Int. J. Heat Mass Transfer* **19**, 613–624.

BUTTERWORTH, D. B. & HEWITT, G. F. 1977 *Two Phase Flow and Heat Transfer.* Oxford University Press.

CLASS, G. 1977 Theoretical investigation of pressure pulsation occurring during steam condensation in the BWR pressure suppression system—computer code KONDAS. KFK 2847.

COLBURN, A. P. 1933–34 Note on the calculation of condensation when a portion of the condensate layer is in turbulent motion. *Trans. AIChE* **30**, 187–193.

COLLIER, J. G. 1972 *Convective Boiling and Condensation.* McGraw-Hill, London.

CUMO, M., FARELLO, G. E. & FERRARI, G. 1978 Direct heat transfer in pressure-suppression systems. *6th Int. Heat Transfer Conf. V.* Paper NR-18, Toronto.

DANCKWERTS, P. V. 1951 Significance of liquid-film coefficients in gas absorption. *J. Indust. Engng Chem.* **43**, 1460–1467.

DOBBINS, W. E. 1956 In *Biological Treatment of Sewage and Industrial Wastes* (Edited by McCabe M. L. and Eckenfelder W. W.), Part 2–1. Reinhold, New York.

FORTESCUE, G. E. & PEARSON, J. R. A. 1967 On gas absorption into a turbulent liquid. *Chem. Engng Sci.* **22**, 1163–1176.

GARDNER, G. C. & CROW, I. G. 1973 Onset of entrainment and mass transfer with a jet directed at a two-phase interface. *Chem. Engng J.* **5**, 267–273.

GREEF, C. P. 1975 A study of condensation of vapor jets injected into subcooled liquid pools. CEGB Rep. RD/B/N3262.

GUNTHER, F. C. & KREITH, F. 1950 Photographic study of bubble formation in heat transfer to subcooled water. Prog. Rep. 4–120, Jet Propulsion Lab., Pasadena, CA.

HIGBIE, R. 1935 The rate of absorption of a pure gas into a still liquid during short periods of exposure. *Trans. AIChE* **31**, 365–389.

KING, C. J. 1966 Turbulent liquid phase mass transfer at a free gas-liquid interface. *Indust. Engng Chem. Fund.* **5**, 1–8.

KISHINEVSKI, M. K. & PANFILOV, A. V. 1949 *J. Appl. Chem. U.S.S.R.* **22**, 118.

KOVASZNAY, L. S. G. 1967 Structure of the turbulent boundary layer. *Phys. Fluids* **10**, Suppl. S25.

KOWALCHUK, W. & SONIN, A. A. 1978 A model for condensation oscillation in a vertical pipe discharging steam into a subcooled water pool. MIT, NUREG/CR-0221.

LAMONT, J. C. & SCOTT, D. S. 1970 An eddy cell model of mass transfer into the surface of a turbulent liquid. *AIChE J.* **16**, 513–519.

LEE, L., JENSEN, R., BANKOFF, S. G., YUEN, M. C. & TANKIN, R. S. 1979 Local condensation rates in cocurrent steam–water flow. In *Nonequilibrium Interfacial Transport Processes* (Edited by Chen J. C. and Bankoff S. G.). ASME, New York.

LEVICH, V. G. 1962 *Physicochemical Hydrodynamics.* Prentice-Hall, Englewood Cliffs, NJ.

LEVY, E. K. & BROWN, G. A. 1967 Investigation of liquid-vapor interaction in a constant-area condensing ejection. AFAPL-TR-67-105, MIT.

LEWIS, W. K. 1916 The principles of counter-current extraction. *J. Indust. Engng Chem.* **8**, 825–833.

LINEHAN, J. H. & GROLMES, M. A. 1970 Condensation of a high velocity vapor on a subcooled liquid jet in stratified flow. *4th Int. Heat Transfer Conf., VI*, paper Cs 2.6, Versailles.

LINEHAN, J. H., PETRICK, M. & EL-WAKIL, M. M. 1969 On the interface shear stress in annular flow condensation. *J. Heat Transfer* **91**, 450–452.

LONGUET-HIGGINS, M. S. 1960 Mass transport in the boundary layer at a free oscillating surface. *J. Fluid Mech.* **8**, 293–306.

MARBLE, F. E. & SHANKAR, R. 1971 Kinetic theory of transient condensation and evaporation at a plane surface. *Phys. Fluids* **14**, 510–516.

MASBERNAT, L. 1977 Étude experimentale du transfert de masse a un interface gaz-liquid. Institut de Mecanique des Fluides, École National Superieure, Toulouse, France.

MERTE, H. 1973 Condensation heat transfer. *Adv. Heat Transfer* **9**, 181–272.

MEYRIAL, P. M., MORIN, M. M., WILCOX, S. J. & ROHSENOW, W. M. 1970 Effect of precision of measurement on reported condensation coefficients for liquid metals—including condensation data on a horizontal surface. *4th Int. Heat Transfer Conf., VI*, Paper Cs 1.1, Versailles.

MICKLEY, H. S., ROSS, R. C., SQUIRES, A. L. & STEWART, W. E. 1954 Heat mass and momentum transfer for flow over a flat plate with blowing or suction. NACA-TN-3208.

MOALEM, D. & SIDEMAN, S. 1973 The effect of motion on bubble collapse. *Int. J. Heat Mass Transfer* **16**, 2321–2329.

MOALEM, D., SIDEMAN, S., ORELL, A. & HETSRONI, G. 1973 Direct contact heat transfer with change of phase: condensation of a bubble train. *Int. J. Heat Mass Transfer* **16**, 2305–2319.

MOTTE, E. I. & BROMLEY, L. A. 1957 Film boiling of flowing subcooled liquids. *Indust. Engng Chem.* **49**, 1921–1928.

PLESSET, M. S. & PROSPERETTI, A. 1978 The contribution of latent heat transport mass transfer in subcooled nucleate boiling. *Int. J. Heat* **21**, 725–734.

REYNOLDS, A. B. & BERTHOUD, 1978 Expansion and collapse of large two-phase bubbles–II. Analysis. In *Advances in Heat and Mass Transfer at Air Water Interfaces*, p. 41. ASME, New York.

ROSE, R. P. 1960 Steam jet pump analysis and experiments. WAPD-TM-227.

SILVER, R. S. & WALLIS, G. B. 1965–66 A simple theory for longitudinal pressure drop in the presence of lateral condensation. *Proc. Inst. Mech. Engrs* **180**, 36–40.

SPALDING, D. B. 1963 *Convective Mass Transfer.* McGraw-Hill, New York.

SURSOCK, J. P. & DUFFEY, R. B. 1978 Condensation of steam bubbles in a subcooled pool. In *Tropics in Two-Phase Flow and Heat Transfer* (Edited by Bankoff S. G.), pp. 135–142. ASME, New York.

THEOFANOUS, T. G., BIASI, L., ISBIN, H. S. & FAUSKE, H. K. 1970 Nonequilibrium bubble collapse: A theoretical study. *Chem. Engng Prog. Symp. Ser.* **66**, 37–47.

THOMAS, R. M. 1979 Condensation of steam on water in turbulent motion. *Int. J. Multiphase Flow* **5**, 1–15.

TSACOYANNIS, J. 1976 Thesis, University Paul Sabatier of Toulouse (Sciences), Toulouse, France.

WHITMAN, W. G. 1923 The two-film theory of gas absorption. *Chem. Met. Engng* **29**, 146–148.

WITTKE, D. D. & CHAO, B. T. 1967 Collapse of vapor bubbles with translatory motion. *J. Heat Transfer* **89**, 17–24.